University of Birmingham

Receptor modelling of airborne particulate matter in the vicinity of a major steelworks site

Taiwo, Adewale; Beddows, David; Calzolai, G.; Harrison, Roy M.; Lucarelli, F.; Nava, S.; Shi, Z.; Valli, G.; Vecchi, R.

Link to publication on Research at Birmingham portal

Receptor Modelling of Airborne Particulate Matter in the Vicinity of a Major Steelworks Site

A.M. Taiwo[1], D.C.S. Beddows[1], G. Calzolai[4,5]
Roy M. Harrison[1]*[†], F. Lucarelli[4,5], S. Nava[5], Z. Shi[1]
G. Valli[2,3], R. Vecchi[2,3]

[1]**Division of Environmental Health & Risk Management**
School of Geography, Earth & Environmental Sciences
University of Birmingham
Edgbaston, Birmingham, B15 2TT
United Kingdom

[2]**Department of Physics**
Università degli Studi di Milano & INFN-Milano
Via Celoria 16, 20133 Milan, Italy

[3]**INFN-Milano**
Via Celoria 16, 20133 Milan, Italy

[4]**Department of Physics and Astronomy**
Università degli Studi di Firenze
Via Sansone 1, 50019 Florence, Italy

[5]**INFN-Firenze**
Via Sansone 1, 50019 Florence, Italy

* Corresponding Author: r.m.harrison@bham.ac.uk

† Also at: Department of Environmental Sciences / Center of Excellence in Environmental Studies, King Abdulaziz University, Jeddah, 21589, Saudi Arabia

31

HIGHLIGHTS

- ➤ Air sampling has taken place at 4 sites around the steelworks.

- ➤ Hourly and daily samples were collected with Streaker and Partisol samplers.

- ➤ ME-2 was applied to both datasets for source apportionment.

- ➤ PM contributions from individual steelworks processes are identified.

- ➤ Steelworks emissions account for 45% of measured PM_{10} mass.

38

ABSTRACT

In this study, the Multilinear Engine (ME-2) receptor model was applied to speciated particulate matter concentration data collected with two different measuring instruments upwind and downwind of a steelworks complex in Port Talbot, South Wales, United Kingdom. Hourly and daily PM samples were collected with Streaker and Partisol samplers, respectively, during a one month sampling campaign between April 18 and May 16, 2012. Daily samples (PM_{10}, $PM_{2.5}$, $PM_{2.5-10}$) were analysed for trace metals and water-soluble ions using standard procedures. Hourly samples ($PM_{2.5}$ and $PM_{2.5-10}$) were assayed for 22 elements by Particle Induced X-ray Emission (PIXE). PM_{10} data analysis using ME-2 resolved 6 factors from both datasets identifying different steel processing units including emissions from the blast furnaces (BF), the basic oxygen furnace steelmaking plant (BOS), the coke-making plant, and the sinter plant. Steelworks emissions were the main contributors to PM_{10} accounting for 45% of the mass when including also secondary aerosol. The blast furnaces were the largest emitter of primary PM_{10} in the study area, explaining about one-fifth of the mass. Other source contributions to PM_{10} were from marine aerosol (28%), traffic (16%), and background aerosol (11%). ME-2 analysis was also performed on daily $PM_{2.5}$ and $PM_{2.5-10}$ data resolving 7 and 6 factors, respectively. The largest contributions to $PM_{2.5-10}$ were from marine aerosol (30%) and blast furnace emissions (28%). Secondary components explained one-half of $PM_{2.5}$ mass. The influence of steelworks sources on ambient particulate matter at Port Talbot was distinguishable for several separate processing sections within the steelworks in all PM fractions.

Keywords: Steelworks; source apportionment; ME-2; hourly resolution; receptor modelling

1. INTRODUCTION

Both acute and chronic exposures to airborne particulate matter (PM) have been associated with adverse effects upon health including premature mortality (Pope and Dockery, 2006). Consequently, the World Health Organisation (WHO, 2006) recommends strict guidelines for airborne particulate matter measured both as PM_{10} and $PM_{2.5}$. Governments around the world are developing and applying abatement strategies to reduce population exposures to particulate matter. The development of cost-effective strategies depends critically upon a quantitative knowledge of the contribution of different sources to airborne particulate matter concentrations. Receptor modelling is a widespread approach to identify emission sources and to resolve their contribution to PM mass (Viana et al., 2008a).

For many years the town of Port Talbot has suffered some of the worst air quality in the United Kingdom (AQEG, 2011). The basic operational steelworks units in Port Talbot are coke making, sintering, blast furnace, basic oxygen furnace and other steel processing units (Passant et al., 2002). Earlier work (Moreno et al., 2004; Dall'Osto et al., 2008; Hayes and Chatterton, 2009) has identified the steelworks as a major contributor to local PM_{10} concentrations and the steelworks units have been recognised as major emission sources of heavy metals such as chromium, copper, lead, cadmium, arsenic, zinc, manganese, iron, nickel, vanadium and selenium (Passant et al., 2002; Moreno et al., 2004; Dall'Osto et al., 2008). However, knowledge has been lacking as to the magnitude of the contribution of the steelworks to airborne PM concentrations as well as the identity of the predominant sources within the steelworks.

The present study focuses on the identification and apportionment of emission sources of particulate matter pollution in the vicinity of the integrated steelworks complex located in Port Talbot. As a complement to previous studies, which used approaches including scanning electron microscopy (Moreno et al., 2004), single particle analysis using an aerosol time of flight mass

spectrometer (Dall'Osto et al., 2008; 2012) and particle size distribution analysis (Taiwo et al.,

2014), the present study has applied the Multilinear Engine (ME-2) receptor model to identify and

apportion emission sources of PM in the study area. The aim was not only to identify the steel

emission profiles, but also to attribute emissions to specific production units in the integrated steel

complex.

2.   MATERIALS AND METHODS

The study area is the coastal industrial town of Port Talbot (51°34'N and 3°46'W) located in South

Wales, UK. The integrated iron and steel facility is the largest steel producer in the UK and one of

the biggest steel producers in Europe, with a production capacity of about 5 million tonnes per year.

It is a complex mixture of stationary source and fugitive emissions associated with the main

processes which consists of iron-making (sintering, blast furnace BF, and raw materials), steel-

making (basic oxygen steel-making BOS and coking) and rolling mills (hot and cold) processing

(Passant et al., 2002). Traditional particle sampling techniques do not have sufficient time

resolution to capture short-lived emission events arising from specific operations; therefore, in this

work we coupled hourly and daily resolution sampling (Lucarelli et al., 2011).

Four monitoring sites [Fire Station (FS), Prince Street (PS), Dyffryn School (DS) and Little Warren

(LW)] were selected within the study area for dichotomous Partisol (daily sampling) samplers,

while Streaker (hourly sampling) samplers were placed at two sites (FS and LW). The Little Warren

sampling location was adopted as the background site, due to the prevailing south-westerly winds

and its typically upwind position (Figure 1). The sites were selected to provide different directions

from steelworks processes in order to assist differentiation of the emission sources.

2.1   Sampling and Analysis

The hourly and daily sampling of PM was achieved through the use of Streaker and Dichotomous Partisol 2025D samplers for a period of 29 days between April 18 and May 16, 2012.

Streaker samples (collected on Nuclepore filters for $PM_{2.5}$ and Kapton foils for $PM_{2.5-10}$) were analysed by Particle Induced X-ray Emission (PIXE) at the 3 MV Tandetron accelerator facility of the INFN-LABEC laboratory in Florence, Italy. Twenty-two elements from sodium to lead were analysed in both fine and coarse Streaker PM samples. Details of the Streaker sampler and PIXE analysis have been extensively reported elsewhere (D'Alessandro et al., 2003; Lucarelli et al., 2014).

Partisol filters (PTFE, Whatman, pore size 1.0 µm) were divided into two equal portions and analysed for water-soluble ions and trace metals. The ionic components were extracted with distilled deionised water and analysed with ICS-2000 (anions) and Dionex DX 500 (cations) ion chromatography instruments. The full procedure for water-soluble ions analysis has been discussed in Yin et al. (2010). The second half PTFE filters were extracted with reverse aqua regia solution as described in Harrison et al. (2003). The extracts were assayed for relevant metals by Inductively Coupled Plasma Mass Spectrometry (ICP-MS, Agilent 7500 Ce). Blank filters were run for all elemental analyses to correct for background levels of elements in the filters used; and also to determine detection limits of the analytes. PM_{10}, fine ($PM_{2.5}$), and coarse ($PM_{2.5-10}$) mass concentration data were obtained for daily samples by weighing.

2.2   Data Analysis

Data were subjected to statistical manipulations including descriptive, analysis of variance, and Duncan Multiple Range Test (DMRT) using SPSS for Windows version 19.0. Source identification and apportionment was carried out with the Multilinear Engine ME-2 receptor model (Paatero, 1999 and 2000).

139 *2.2.1   Brief description of ME-2 model*

140 ME-2 is a least squares program for solving multi-linear problems. Specifically, it solves models

141 where the data values are fitted by sums of products of unknown factor elements (Paatero, 2000).

142 For bilinear problems it takes the form $X = G \cdot F + E$, where X is the known n by m matrix of the m

143 measured chemical species in n samples; G is an n by p matrix of factor contributions to the

144 samples; F is a p by m matrix of species concentrations in the factor profile. G and F are factor

145 matrices to be determined and they are constrained to non-negative values only. E is defined as a

146 residual matrix i.e. the difference between the measurement X and the model $Y = G \bullet F$ as a

147 function of G and F.

148

149 One advantage in using ME-2 is that a priori information can be added as linear constraints in the

150 object function to be minimized instead of using the generic rotational tools available in Positive

151 Matrix Factorization (Paatero and Hopke, 2009; Amato et al., 2009; Amato and Hopke, 2012; and

152 therein cited literature).

153

154 In this work, the datasets analysed with ME-2 comprised only normal variables, defined according

155 to the signal-to-noise criterion reported in Paatero and Hopke (2003).

156

157 Uncertainties for Partisol daily samples were calculated using the formula adopted by Viana et al.

158 (2008b) as $0.1 \cdot C + MDL/3$; where C is the concentration and MDL is the method detection limit. All

159 below-detection-limit data were treated equally by replacing with $1/2 \cdot MDL$ and their corresponding

160 uncertainties calculated as $5/6 \cdot MDL$. Missing data were replaced with the geometric mean values

161 and then down-weighed assigning them an uncertainty calculated as $4 \cdot C$, with C being the

162 concentration value (Polissar et al., 1998). Streaker hourly data were pre-treated according to

163 Polissar et al. (1998) as the below-detection limit data and experimental uncertainty (comprising

164   counting statistics error, uncertainty on the measurement standard and spectra fitting errors) were

165   available for each hourly entry. MDLs for daily and hourly data are reported in Table 1.

166

167   ME-2 analysis on the hourly data refers to the parallel sampling periods at LW and FS sites (i.e.

168   about 300 hours in total), where the fine and the coarse PM fractions were summed up obtaining the

169   PM_{10} elemental dataset to be analysed with ME-2. In this work, the high-resolution dataset was

170   exploited to retrieve a detailed identification of the different sources affecting PM_{10} levels

171   registered in the steelworks area, especially focusing on different iron-making and steel-making

172   processes and aiming at improving the source apportionment with daily samples.

173

174   Partisol daily data collected at different sites in the steelworks area were pooled together in order to

175   get a dataset suitable for multivariate analysis (N=99). This approach is supported by the similarity

176   in the major sources impacting on the LW and FS sites as shown by the ME-2 analysis on the

177   hourly data (see section 3.2). It is worth noting that sampling at the four sites occurred almost in

178   parallel (i.e. during the same days) and the sampling stations were all around the steelworks area;

179   thus, pooling all the data together might have helped in disentangling sources which at one single

180   site would have been collinear. As a matter of fact, the average source apportionment is referred to

181   the investigated area as a whole.

182

183   Following Amato and Hopke (2012), in this work two physical constraints deriving from mass

184   conservation were incorporated in the analysis of daily data in order to improve the obtained

185   solution for daily samples: 1) the single source contributions on a given day must be smaller than

186   PM mass concentration on the same day; 2) for each source, the sum of factor profile must be less

187   than unity.

188

189

3. RESULTS AND DISCUSSION

3.1 Elemental and Ion Concentrations for Daily PM Data

Table 2 shows the mean concentrations of mass, ionic and metal components from 29 days of

Partisol data collected at the four monitoring sites, with their percentages in the total PM mass.

During the monitoring campaign PM_{10} daily mass concentrations exceeded the 50 µg/m^3 limit value

on only one occasion at the FS site. In total, secondary aerosol components (nss-SO_4^{2-}, NO_3^- and

NH_4^+) constituted 43% of measured $PM_{2.5}$ at FS, 30% at PS, 54% at DS and 67% at LW. Na^+ and

Cl^- were also significant components of $PM_{2.5}$ (7-14%) and especially of $PM_{2.5-10}$ (16-34%) at all

monitoring sites. Among heavy metals, the most abundant in $PM_{2.5}$ were Fe and Zn at all sites and

in $PM_{2.5-10}$ only Fe showed relevant contributions, i.e. ranging from 5 to 9%, with the highest

percentages at FS and PS (i.e. the nearest to the blast furnace plant and to major roads). In both the

fine and coarse PM fractions K^+, Mg^{2+}, Ca^{2+}, and Al contributed a few percent to PM mass.

The average wind rose registered during the investigated period is reported in Figure 2.

Meteorological data are calculated for the Margam station (next to the Fire Station site) belonging

to the Automatic Urban and Rural Network by the Department for Environment, Food and Rural

Affairs (DEFRA, http://uk-air.defra.gov.uk/data/).

3.2 Source Identification with Streaker Hourly Data

Direct information on the mass on Streaker samples is not available so that ME-2 results can be

used for a detailed source identification (i.e. the factor profiles will be given in arbitrary units) but

not for obtaining a complete source apportionment (D'Alessandro et al. 2003).

ME-2 analysis (base case) gave meaningful results for the 6-factor solution; it showed very good

correlations (R^2=0.80-0.99) between measured and modelled elemental concentrations and elements

216   were reconstructed within 20% (i.e. modelled to measured concentration ratio in the range 0.8-1) at

217   both sites. Exceptions were Cu and Pb (and also Ti at LW). The Cu concentrations were fairly well

218   reconstructed (i.e. in the worst case within 2% with R^2=0.99) considering the 7-factor solution

219   where Cu appeared as a unique factor. On the contrary, Pb peaks were always poorly reconstructed

220   also when considering a higher number of factors.

221

222   The 6-factor solution for PM_{10} (i.e. fine + coarse PM fraction) collected at the Fire Station (main

223   site) and Little Warren (coastal site) stations is reported in Figure 3. Chemical profiles (bars in

224   arbitrary units) and explained variation values (EVF) are represented.

225

226   It is worth noting that in almost all cases the factors showed fairly similar profiles and EVF at both

227   sites pointing to the same sources impacting on the areas adjacent to the steelworks. The major

228   difference was found for the Steel 2 factor, as will be explained in the following.

229

230   Polar plots given in Figure 4 (LW site on the left and FS on the right) were also inspected for a

231   more effective discrimination of different emission sources. Polar plots derive from the ME-2

232   analysis of the Streaker hourly data and show the wind direction (angle from centre) and wind speed

233   (distance from centre) dependence of the resolved factors attributed to emission sources (Carslaw

234   and Ropkins, 2012; Carslaw, 2013).

235

236   Blast furnaces (BF), sinter plant, basic oxygen steel-making (BOS) plant, coke-making plant,

237   rolling mills, and ore stockyards are located in a southerly and westerly sector from the FS (170-

238   270°) site at Port Talbot (see Figure 1). This is reflected in the directional pattern of all factors

239   related to steelworks emissions reported in this work. From the LW site, the steel industry is located

240   within the south and south-east sectors (100-180°). The majority of factors and especially those

241   associated with steelworks emissions at the LW site show an association with this sector.

242   Factor 1 is labelled as "Marine Aerosol" according to the high EVF values and contributions of Cl,

243   Na, and Mg, which are typical markers for sea salt (Viana et al., 2008a; and reference therein). As

244   expected, the marine factor (Figure 4a) is strongly associated with westerly winds and its impact

245   can be seen at both sites.

246

247   The high EVF values for Fe and Mn in factor 2 and the dominant Fe concentration in the chemical

248   profile suggest apportionment to the iron-making plant (Dall'Osto et al., 2008; Mazzei et al., 2008)

249   and especially to the blast furnace (BF) emissions; this factor is named "Steel 1 (BF)". The removal

250   of the S content in the pig iron-making process is facilitated by Mn and lime; the former can be in

251   the iron mineral or is specifically inserted as auxiliary mineral. Lime is generally produced by

252   limestone ($CaCO_3$) decomposition or alternatively it is introduced with the fluxing agent. The latter

253   process can contribute to Ca found in the chemical profile of factor 2. The polar plots (Figure 4b)

254   show that the Steel 1 contributions come from the BF area at both locations.

255

256   Factor 3 is named "Steel 2 (BOS)" due to the presence of Zn as the marker element (i.e. with the

257   highest EVF value). Indeed, the use of galvanised scrap in the BOS has been stated to increase Zn

258   concentrations in the steelworks processing section (Oravisjarvi et al., 2003; Hleis et al., 2013).

259   This is the factor with the largest difference in the chemical profiles obtained at LW and FS as there

260   is a not negligible contribution of S at LW and Fe at FS site; although their EVF values are of very

261   little importance here. A likely S-rich source contribution at the LW site is from shipping emissions

262   of sulphur dioxide on the adjacent waterway and in the in-shore and off-shore harbours (see Figure

263   1). Previous work has reported the accumulation of sulphate and nitrate on metal-rich particles (e.g.

264   forming $ZnSO_4$ and $PbSO_4$ particles) as well as on sea salt or soil dust particles (e.g. forming

265   Na_2SO_4 and $NaNO_3$ particles) (Sullivan et al., 2007; Marris et al., 2012; Perrone et al., 2013). The

266   other relevant difference is the presence of Fe in the FS profile that could be due to a meteorological

267   collinearity between the BOS and the BF plant. Further investigation on this Fe content is needed to

268   disentangle the contribution of these different sources. The polar plots (Figure 4c) are consistent

269   with the BOS location in respect to the measuring sites and show somehow a narrower directional

270   sector, pointing at the existence of pollution plumes from this plant.

271

272   In factor 4, sulphur is the dominant element in the profile at both sites. Also Cu and Pb at LW and

273   Pb at FS show EVF values larger than 0.3. The high S concentration can be related to coke making

274   emissions rich in SO_2; Pb and SO_2 were attributed to coking emissions also in previous work (e.g.

275   Pacyna, 1987; Pancras et al., 2013). The SO_2 emissions can promote sulphate aerosol formation as

276   well as the accumulation of sulphate on metals emitted by different iron and steel-making processes

277   as reported above. In addition to sources located in the steelworks area, the polar plots for this

278   factor (Figure 4d) at both sites show contributions coming from the east and the centre of the plots.

279   The EVF values of S, Cu, and Pb together with the polar plots for factor 4 suggest a possible

280   association with traffic emissions (Pant and Harrison, 2013; and references therein). Likely these

281   are non-exhaust and exhaust emissions due to both heavy duty traffic in the steelworks area, which

282   is estimated as 25,000 vehicle movements a day, and traffic on major roads due to the M4 and A48

283   located nearby (DfT, 2012). This factor is called "Steel 3 (coking) + Traffic", where Steel 3

284   comprises primary and secondary (i.e. metals and sulphates) contributions from the coking plant.

285

286   Factor 5 is enriched in Na and S and shows EVF values higher than 0.3 for Na, Mg, Al at both sites

287   and additionally S at FS site. The polar plots for this factor (Figure 4e) point at a widespread source

288   with higher contributions coming from the south-west (and to a lesser extent from the east) at LW

289   and west (and to a lesser extent from the south-east) at FS. The spatial distribution and the chemical

290   profile of this factor suggest the association with "background aerosol" with a mixed marine (i.e.

291   aged aerosol) and mineral origin. Indeed, the Mg-to-Na ratio at both sites (0.12-0.14) is consistent

292   with the expected (0.12) seawater value (Seinfeld and Pandis, 1998). Moreover, Marris et al. (2012)

293   during near-field transport of industrial plumes attributed the presence of Na_2SO_4 and $NaNO_3$

11

294   particles to aged sea-salts due to the reaction of NaCl with gaseous anthropogenic pollutants like

295   SO_2 and NO_x producing a Cl loss. Mineral components like aluminosilicates, calcite, gypsum and

296   metallic elements were also found by Marris et al. (2012) in binary mixtures with marine particles

297   resulting from the mixing with dust of continental origin. In our study, re-suspended dust in the

298   steelworks area could give the soil-related contribution and likely the hot-spots observed in the

299   polar plots.

300

301   The factor 6 profile is characterised by the presence of Al, Si, and Ca at both sites. In Figure 3, EVF

302   values larger than 0.3 for Al, Si, Ca, Ti at LW and Al, Si, Cu at FS can be seen. The polar plots

303   (Figure 4f) show high contributions from the westerly, south-westerly and north-westerly directions

304   at the FS site and from the west and south-east at LW thus pointing to different contributing

305   sources. Investigations performed on stack emissions from sintering units (Marris et al., 2012;

306   Setyan et al., 2013) report that emissions coming especially from the cooling area of the sintering

307   plant largely consist of internally mixed aluminosilicates/metallic particles thus suggesting an

308   association between factor 6 and sinter plant emissions (Steel 4). This is consistent with the sinter

309   plant unit location (see Figure 1). Considering the factor profile and EVF values, a contribution due

310   to slag processing cannot be excluded as Proctor et al. (2000) report that BF slag mainly consists of

311   silica and alumina from the iron ore and Ca, Mg are primarily from the added flux. Sometimes slags

312   are also used as road materials, landfill cover material, cement additive and other applications. At

313   FS site there is also a high EVF for Cu (not observed at LW) that could be due to a very local road

314   dust contribution as FS is next to major roads. Finally, the high concentration coming from the west

315   at both sites can be an indication of a contribution by mineral elements re-suspended from the

316   nearby sandy seashore. For sake of brevity, this factor is tentatively labelled as "Steel 4 (sintering)

317   + Dust".

318

319   In Figure 5 the temporal patterns of the factors resolved by ME-2 are represented in arbitrary units

320   for the FS and LW sites. It is worth noting that the marine aerosol source shows a fair agreement in

321   the temporal patterns at the two sites while the steelworks-related sources are characterised by sharp

322   peaks occurring at different times at the two locations. The background aerosol source has a more

323   irregular character likely due to the behaviour of re-suspended soil-related and aged marine aerosol

324   in connection with different wind regimes. The temporal behaviours observed highlight the need for

325   high resolution techniques when studying such a kind of emissions.

326

327   **3.3   Source apportionment for Partisol Daily Data**

328   Figures 6a-c show the chemical profiles and explained variation values obtained with ME-2 for

329   Partisol daily PM_{10}, $PM_{2.5}$, and $PM_{2.5-10}$ data. Figures 7a-c show the corresponding average source

330   apportionment for the steelworks area. It is worth noting that in this case the compositional data and

331   mass concentrations from 4 different stations were pooled together. However, the analysis of the

332   Streaker hourly data reported in the previous section indicated that there are no significant

333   differences in the sources impacting in the steelworks area; therefore, the pooling of the

334   compositional data can be performed in order to get a more robust source identification.

335

336   The optimal ME-2 solution showed 6 factors for PM_{10} (in agreement with the sources resolved in

337   the hourly datasets), 7 factors for $PM_{2.5}$, and 6 factors for $PM_{2.5-10}$. The Q_{main}-to-Q_{teo} ratio was 1.5,

338   2, and 1.8 for PM_{10}, $PM_{2.5}$, and $PM_{2.5-10}$, respectively. This ratio between Q values is often used as

339   an indicator for a good fit of the data (Belis et al., 2013). The computed versus measured PM_{10} mass

340   was higher than 0.95 in all cases showing a fairly good correlation (R^2=0.92 and 0.95 for PM_{10} and

341    $PM_{2.5-10}$; R^2=0.73 for $PM_{2.5}$). The factors related to iron- and steel-making emissions were labelled,

342   as far as possible, with the same names given in the solution obtained for the hourly data.

343

344   The high EVF values for Na, Mg, and Cl and the profile in factor 1 for PM_{10} (Figure 6a) point at the

345   association with the "Marine aerosol" source. It seems specifically a fresh marine contribution as

346   the Cl-to-Na ratio is 1.7 and the Mg-to-Na ratio is 0.10, in good agreement with the average

347   composition of the sea salt (Seinfeld and Pandis, 1998). However, the profile is enriched in Fe, Ca,

348   and Al which are likely due to a meteorological collinearity with the industrial emission sources;

349   indeed, to reach the FS, DS, and PS sites the marine air masses overpass the steelworks area. In the

350   average source apportionment (Figure 7a) this factor accounts for 28% of the PM_{10} mass. The

351   marine aerosol source is also present in the ME-2 solutions obtained for the fine and the coarse PM

352   fractions separately (Figures 6b and 6c) accounting for 20% and 30%, respectively (Figures 7b and

353   7c). In the fine fraction the Cl-to-Na ratio is about 1.2 (vs. 2 in the coarse fraction) suggesting that

354   aged marine aerosol is likely to be the contributor in the smallest PM fraction.

355

356   All PM fractions show high EVF values for Cu, Sb, and Ba in factor 2 for PM_{10}, which is labelled

357   as "Traffic". These trace metals are a signature of road traffic especially from brake wear

358   (Sternbeck et al., 2002; Thorpe and Harrison, 2008; Pant and Harrison, 2013). It accounts for 16%

359   of the PM_{10} mass. The Cu/Sb ratio is 3.2 to be compared to 4.6 ($\pm$ 2.3) proposed by Sternbeck et al.

360   (2002) for brake wear particles. Considering ME-2 results presented in Figures 6b and 6c for the

361   traffic factor, this ratio ranges from 2.3 in the fine PM fraction to 4.9 in the coarse PM fraction.

362

363   In factor 3, Fe and Mn show the highest EVF values in all PM fractions. Also Ca in PM_{10} and Ni

364   and Pb in $PM_{2.5-10}$ show EVF values higher than 0.3. Fe, Mn, and Ca are typical of blast furnace

365   (BF) emissions as already discussed in the hourly data results and the factor is called "Steel 1",

366   accordingly. Fe has been generally observed at all the processing units of integrated steel

367   production (Oravisjarvi et al., 2003; Machemer, 2004; Moreno et al., 2004; Connell et al., 2006;

368   Tsai et al., 2007; Dall'Osto et al., 2008; Hleis et al., 2013). However, the recent source profile study

369   of integrated steel facilities by Hleis et al. (2013) showed a more elevated Fe concentration from the

370   BF relative to other steelworks units. The average contribution of the Steel 1 source to PM_{10} is 19%

371   and it is by far the largest one among those related to the steelworks activities. Steel 1 contribution

372   explains 9% and 28% of the fine and coarse PM mass, respectively.

373

374   For all PM fractions EVF values in factor 4 are dominated by Zn and Cd; in addition, Pb is present

375   in this factor with its highest concentration when compared to other factors. Zn has been already

376   mentioned as the marker element of BOS emissions and Pb was found in the corresponding profile

377   obtained with the Streaker hourly dataset. The presence of K and Cl in the chemical profile of this

378   factor for PM_{10} and $PM_{2.5}$, known as major components in sinter plant emissions, together with the

379   high EVF value for Cd point at the sinter plant unit as the most likely additional contributor

380   (Oravisjarvi et al., 2003). Therefore, this factor is named "Steel 2 (BOS) + Steel 4 (sinter plant)". It

381   explains on average 3% of the PM_{10} mass, 5% of the fine fraction mass and 3% of the PM coarse

382   mass.

383

384   Factor 5 in PM_{10} has similarities with factor 5 resolved in the hourly resolution data so that it is

385   labelled accordingly as "background aerosol". This source contributes 11% to PM_{10} mass (6% in

386   the fine fraction and 10% in the coarse PM).

387

388   Factor 6 for PM_{10} is characterised by the relevant presence of sulphate, nitrate, and ammonium in

389   the chemical profile with high EVF values thus relating it to secondary components of aerosol. In

390   this factor the sulphate-to-ammonium ratio is 2.8 suggesting that sulphate is mainly in the form of

391   ammonium sulphate; the nitrate in the profile is likely to be attributed to other chemical compounds

392   (e.g. $NaNO_3$). Metals in the source profile suggest that a contribution coming from one of the

393   production units in the steelworks area is superimposed. Coke-making is likely to be the emission

394   source because of the concomitant presence of Pb and sulphate, similarly to what was found for the

15

395   hourly resolution results. This composite factor for PM_{10} is labelled as "Secondary aerosol + Steel

396   3" and on average it accounts for about 22% of the PM_{10} mass.

397

398   As mentioned before, for $PM_{2.5}$ the optimal ME-2 solution is the 7-factor one (Figure 6b), which

399   separates the contributions from sulphates and nitrates accounting for 27% and 20%, respectively

400   (Figure 7b). The sulphate-to-ammonium ratio is 2.2 in factor 6 and the nitrate-to-ammonium ratio is

401   4.6 in factor 7 indicating the possibility of having ammonium sulphate and nitrate in the fine PM

402   fraction. Again, the presence of heavy metals in the profile of factor 6 –especially Pb – together

403   with sulphates might be due to coking. In Figure 6b, factor 6 and factor 7 for $PM_{2.5}$ are called

404   "Ammonium Sulphate + Steel 3" and "Ammonium Nitrate", respectively.

405

406   In factor 6 for the $PM_{2.5-10}$ fraction (Figure 6c) nitrates and sulphates appear together with very high

407   sulphate-to-ammonium and nitrate-to-ammonium ratios (i.e. 18 and 27, respectively) thus excluding

408   the presence of ammonium nitrate and sulphate in the PM coarse fraction. This factor is named

409   "Sulphates + Nitrates" and other chemical forms of sulphates and nitrates must be considered (as

410   mentioned above in the text). Also in this case, the presence of metals in the profile is indicative of

411   additional contributions coming from the steelworks primary emissions. This factor accounts for

412   13% of the coarse PM mass (Figure 7c).

413

414   **4.   CONCLUSIONS**

415   The hourly data collected at Port Talbot captured the peculiarities of different emissions from the

416   integrated iron and steel-making facility and were effective in resolving contributions from different

417   steelworks units that the daily data could not always detect due to the short time characterising these

418   emissions. Moreover, the hourly resolution demonstrated high metal concentrations lasting a few

419   hours which may lead to an exposure problem in this area.

420

421   The receptor model analysis of daily and hourly data collected at Port Talbot has allowed

422   identification of 6 factors for PM_{10} and $PM_{2.5-10}$ and 7 factors for $PM_{2.5}$. The polar plots for the ME-

423   2 profiles of the hourly data were helpful to resolve sources with similar chemical signatures.

424   Additionally, the polar plots were able to identify the directional locations of different steel

425   processing units resolved by ME-2. Contributions not clearly singled out using the hourly data

426   alone (e.g. secondary contributions or traffic) are mainly ascribed to the lack of suitable markers; it

427   is thus desirable in future work to combine hourly resolution data on different chemical components

428   (e.g. more elements, ions, carbonaceous components). Overall the steelworks emissions assigned to

429   blast furnaces (Steel 1), basic oxygen furnace steelmaking plant (Steel 2), and sinter unit (Steel 4)

430   account for 23% of PM_{10} mass. Other source contributions in the area are marine aerosol (28%),

431   secondary aerosol and coking (Steel 3) (22%), traffic emissions (16%), and background aerosol

432   (11%). The major contributor among the various steelwork units are the blast furnaces accounting

433   for one-fifth of the PM_{10} mass. It is interesting to note that large source contributions to the coarse

434   PM fraction come from Steel 1 (BF) accounting on average for 28% of the measured mass

435   concentration (vs. 9% in the fine fraction). As for $PM_{2.5}$, not surprisingly, the largest contribution is

436   given by secondary components (i.e. ammonium sulphate and nitrate), which explain about half of

437   the PM fine fraction mass.

438

439   By and large, both daily and hourly ME-2 profiles are complementary and effective in identifying

440   and apportioning pollution sources. The chemical profiles for both daily and hourly data have been

441   able to separate contributions from different steelworks units, which have not been previously

442   reported in any published literature known to us.

443

454 **REFERENCES**

455 Amato F, Pandolfi M, Escrig A, Querol X, Alastuey A, Pey J, Prez N, Hopk, PK. Quantifying road
456 dust resuspension in urban environment by Multilnear Engine: A comparison with PMF2. Atmos
457 Environ 2009;43:2770-2780.

458 Amato F, Hopke PK. Source apportionment of the ambient PM2.5 across St. Louis using
459 constrained positive matrix factorization. Atmos Environ 2012;46:329-337.

460 AQEG. Understanding PM_{10} in Port Talbot. Advise note prepared for Department of Environment,
461 Food and Rural Affairs: Scottish, Welsh Assembly Government, and Department of the
462 Environment, Northern Ireland, 2011.

463 Belis, C.A., Larsen B.R., Amato, F., El Haddad, I., Favez, O., Harrison, R.M., Hopke, P.K., Nava,
464 S., Paatero, P., Prévôt, A., Quass, U, Vecchi, R., Viana, M. European Guide on Air Pollution
465 Source Apportionment with Receptor Models, JRC Reference Reports EUR26080 EN, 2013.

466 Carslaw DC, Ropkins K. Openair — an R package for air quality data analysis. Environmental
467 Modelling & Software 27/28, 52-61, 2012.

468 Carslaw DC. The Openair manual — open-source tools for analysing air pollution data. Manual for
469 version 0.8-0, King's College London, 2013.

470 Connell DP, Winter SE, Conrad VB, Kim M, Crist KC. The Steubenville Comprehensive Air
471 Monitoring Program (SCAMP): Concentrations and solubilities of PM2.5 Trace elements and their
472 implications for source apportionment and health research. JAWMA 2006;56:1750-1766.

473 D'Alessandro A, Lucarelli F, Mandò PA, Marcazzan G, Nava S, Prati P, Valli G, Vecchi R,
474 Zucchiatti A. Hourly elemental composition and sources identification of fine and coarse PM10
475 particulate matter in four Italian towns, J Aerosol Sci 2003;34:243-259.

476 Dall'Osto M, Booth A, MJ, Smith W, Fisher R, Harrison RM. Study of the size distributions and the
477 chemical characterization of airborne particles in the vicinity of a large integrated steelworks.
478 Aerosol Sci Technol 2008;42:981-991.

479 Dall'Osto M, Drewnick F, Fisher R, Harrison RM. Real-Time measurements of non-metallic fine
480 particulate matter adjacent to a major integrated steelworks. Aerosol Sci Technol 2012;46:639-653.

481 DfT. Neath Port Talbot: Total traffic on major roads (thousand vehicle miles), 2000 to 2011, 2012.
482 www.dft.gov.uk/traffic-counts/area.php?region=Wales&la=Neath+Port+Talbot. *Accessed:27/10/12.*

483 Harrison RM, Jones AM, Lawrence RG. A pragmatic mass closure model for airborne particulate
484 matter at urban background and roadside sites. Atmos Environ 37;2003:4927-4933.

485 Hayes E, Chatterton T. An independent review of monitoring measures undertaken in Neath Port
486 Talbot in respect of particulate matter (PM_{10}), Report prepared for the Welsh Assembly
487 Government by the University of the West of England, Bristol, 2009.

488 Hleis D, Fernandez-Olmo I, Ledoux F, Kfoury K, Courcot L, Desmonts T, Courcot D,.Chemical
489 profile identification of fugitive and confined particle emissions from an integrated iron and
490 steelmaking plant. J Hazard Mater 2013;250-251:246-255.

491 Lucarelli F, Nava S, Calzolai G, Chiari M, Udisti R, Marino F. Is PIXE still a useful technique for
492 the analysis of atmospheric aerosols? The LABEC experience. X-Ray Spectrom 2011;40:162-167.

493 Lucarelli F, Calzolai G, Chiari M, Giannoni M, Mochi D, Nava S, Carraresi L. The upgraded
494 external-beam PIXE/PIGE set-up at LABEC for very fast measurements on aerosol samples. Nucl
495 Instr Meth in Phys Res B: Beam Interactions with Materials and Atoms 2014;318:55-59.

496 Machemer SD. Characterization of airborne and bulk particulate from iron and steel manufacturing
497 facilities. Environ SciTechnol 2004;38:381-389.

498 Marris H, Deboudt K, Augustin P, Flament P, Blond F, Fiani E, Fourmentin M, Delbarre H. Fast
499 changes in chemical composition and size distribution of fine particles during the near-field
500 transport of industrial plumes. Sci Total Environ 2012;427-428:126-138.

501 Mazzei F, D'Alessandro A, Lucarelli F, Nava S, Prati P, Valli G, Vecchi R. Characterization of
502 particulate matter sources in an urban environment. Sci Total Environ2008;401:81-89.

503 Moreno T, Jones TP, Richards RJ. Characterisation of aerosol particulate matter from urban and
504 industrial environments: examples from Cardiff and Port Talbot, South Wales, UK. Sci Total
505 Environ 2004;334-335:337-346.

506 Oravisjarvi K, Timonen,KL, Wiikinkoski T, Ruuskanen AR, Heinanen K., Ruuskanene J. Source
507 contributions to PM$_{2.5}$ particles in the urban air of a town situated close to a steel works. Atmos
508 Environ 2003;37:1013-1022.

509 Paatero P. The multilinear engine - a table-driven least squared program for solving multilinear
510 problems, including the n-way parallel factor analysis model. University of Helsinki, Department of
511 Physics, 1999.

512 Paatero P. User's guide for the Multilinear Engine program `ME2' for fitting multilinear and quasi-
513 multilinear models, 2000.

514 Paatero P, Hopke PK. Discarding or downweighting high-noise variables in factor analytic models.
515 Anal Chim Acta 2003;490:277-289.

516 Paatero P, Hopke PK. Rotational tools for factor analytic models. J. Chemometr 2009;23:91-100.

517 Pacyna JM. Atmospheric emissions of arsenic, cadmium, lead and mercury from high temperature
518 processes in power generation and industry. In: Lead, Mercury, Cadmium and Arsenic in the
519 Environment, edited by Hutchinson TC and Meema KM, John Wiley and Sons, 1987.

520 Pancras JP, Landis MS, Norris GA, Vedantham R, Dvonch JT. Source apportionment of ambient
521 fine particulate matter in Dearborn, Michigan, using hourly resolved PM chemical composition
522 data. Sci Total Environ 2013;448:2-13.

523 Pant P, Harrison RM. Estimation of the contribution of road traffic emissions to particulate matter
524 concentrations from field measurements: A review. Atmos Environ 2013;77:78-97.

525 Passant NR, Peirce M, Rudd HJ, Scott DW, Marlowe I, Watterson JD. UK Particulate and Heavy
526 Metal Emissions from Industrial Processes. A report produced for the Department for Environment,
527 Food & Rural Affairs, the National Assembly for Wales, the Scottish Executive and the Department
528 of the Environment in Northern Ireland. AEAT-6270 Issue 2, 2002.

529 Perrone, MR, Becagli S, Orza JAG, Vecchi R, Dinoi A, Udisti R, Cabello M. The impact of long-
530 range-transport on PM1 and PM2.5 at a Central Mediterranean site. Atmos Environ 2013;71:176-
531 186.

532 Polissar AV, Hopke PK, Paatero P, Malm WC, Sisler JF.. Atmospheric aerosol over Alaska 2.
533 Elemental composition and sources. J Geophys Res 1998;103:19045-19057.

534 Pope CA, Dockery DW. Health effects of fine particulate air pollution: Lines that connect. JAWMA
535 2006;56:709-742.

536 Proctor DM, Fehling KA, Shay EC, Wittemborn JL, Green JJ, Avent C, Bigham RD, Connolly M,
537 Lee B, Shepker TO, Zak MA. Physical and chemical characteristics of blast furnace, basic oxygen
538 furnace, and electric arc furnace steel industry slags. Environ Sci Technol 2000;34:1576-1582.

539 Sciare, J., Bardouki, H., Moulin, C., Mihalopoulos, N. (2003). Aerosol sources and their
540 contribution to the chemical composition of aerosols in the Eastern Mediterranean Sea during
541 summertime. Atmos. Chem. Phys., 3, 291–302.

542 Seinfeld JH, Pandis SN., Atmospheric Chemistry and Physics—From Air Pollution to Climate
543 Change. John Wiley, Hoboken, N.J., 1998

544 Setyan,A, Flament P, Locoge N, Deboudt K, Riffault V, Alleman LY, Schoemaecker C, Arndt J,
545 Augustin P, Blond F, Blondel A, Cazier F, Delbarre H, Dewaele D, Dewalle P, Fourmentin M,
546 Genevray P, Healy RM, Le Louer P, Leonardis T, Marris H, Mbengue S, Wenger J.
547 Characterization of fine particles in the near-field of a metallurgy plant: overview of the NANO-
548 INDUS project. European Aerosol Conference EAC2013, Prague, 2013.

549 Sternbeck J, Sjodin A, Andreasson,K. Metal emissions from road traffic and the influence of
550 resuspension - results from two tunnel studies. Atmos Environ 2002;36:4735-44.

551 Sullivan RC, Guazzotti SA, Sodeman DA, Prather KA. Direct observations of atmospheric
552 processing of Asian mineral dust. Atmos Chem Phys 2007;7:1213-1236.

553
554 Taiwo AM, Beddows DCS, Shi Z, Harrison RM. Mass and number size distributions of particulate
555 matter components: Comparison of an industrial site and an urban background site. Sci Total
556 Environ 2014;475:29-38.

557 Thorpe A, Harrison RM. Sources and properties of non-exhaust particulate matter from road traffic:
558 A review. Sci Total Environ 2008;400:270-282.

559 Tsai J-H, Lin K-H, Chen C-Y, Ding J-Y, Choa C-G, Chiang H-L,.. Chemical constituents in
560 particulate emissions from integrated iron and steel facility. J Hazard Mater 2007;147:111-119.

561 Viana M, Kuhlbusch TAJ, Querol X, Alastuey A, Harrison RM, Hopke PK, Winiwarter W, Vallius
562 M, Szidat S, Prévôt ASH, Hueglin C, Bloemen H, Wåhlin P, Vecchi R, Miranda AI, Kasper-Giebl
563 A, Maenhaut W, Hitzenberger R. Source apportionment of PM in Europe: a review of methods and
564 results. J Aerosol Sci 2008a;39:827-849.

565 Viana M, Pandolfi M, Minguillo MC, Querol X, Alastuey A, Monfort E, Celades I. Inter-
566 comparison of receptor models for PM source apportionment: Case study in an industrial area.
567 Atmosc Environ 2008b;42:320-3832.

568 WHO. WHO Air quality guidelines: Global update 2005. World Health Organization, Copenhagen.
569 Denmark, 2006.

570 Yin J, Harrison RM, Chen Q, Rutter A, Schauer JJ. Source apportionment of fine particles at urban
571 background and rural sites in the UK atmosphere. Atmos Environ 2010;44:841-851.

572

TABLE LEGENDS

Table 1: Minimum Detection Limits (MDL) for daily and hourly data.

Table 2: Mean, standard deviation and percentage composition of water soluble ion and metal concentrations of daily $PM_{2.5}$ and $PM_{2.5-10}$ concentrations in Port Talbot.

FIGURE LEGENDS

Figure 1: Map of study area

Figure 2: Average wind rose for Margam station (Fire Station site) in Port Talbot during the campaign period

Figure 3: 6-Factor solution resolved by ME-2 for hourly PM_{10} (i.e. fine + coarse PM fraction) collected at Little Warren (on the left) and Fire Station (on the right). Chemical profiles are represented as bars (in arbitrary units) and the explained variation values (EVF) as dots.

Figure 4: Bi-variate polar plots of hourly data in ME-2 factor contributions. (a) Marine aerosol; (b) Steel 1; (c) Steel 2; (d) Secondary + Traffic; (e) Background aerosol; (f) Steel 4 + Dust. LW site on the left; FS on the right.

Figure 5: Hourly temporal patterns of factor contributions obtained in the ME-2 6-factor solution.

Figure 6a: 6-Factor solution resolved by ME-2 for PM_{10} (daily data) in the steelworks area. Chemical profiles are represented as bars (in ng/ng) and the explained variation as dots.

Figure 6b: 7-Factor solution resolved by ME-2 for $PM_{2.5}$ (daily data) in the steelworks area. Chemical profiles are represented as bars (in ng/ng) and the explained variation as dots.

Figure 6c: 6-Factor solution resolved by ME-2 for $PM_{2.5-10}$ (daily data) in the steelworks area. Chemical profiles are represented as bars (in ng/ng) and the explained variation as dots.

Figure 7a: Source apportionment for PM_{10} (daily data) in the steelworks area.

Figure 7b: Source apportionment for $PM_{2.5}$ (daily data) in the steelworks area.

Figure 7c: Source apportionment for $PM_{2.5-10}$ (daily data) in the steelworks area.

610 **Table 1**: Minimum Detection Limits (MDL) for daily and hourly data.
611

Daily samples (Partisol)			Hourly samples (Streaker)		
Species	$PM_{2.5}$ (ng m^{-3})	$PM_{2.5-10}$ (ng m^{-3})	Species	$PM_{2.5}$ (ng m^{-3})	$PM_{2.5-10}$ (ng m^{-3})
Cl^-	42	31	Na	42	25
NO_3^-	34	26	Mg	22	13
SO_4^{2-}	200	150	Al	17	10
Na+	127	101	Si	14	10
NH_4^+	33	26	S	15	12
K^+	2	2	Cl	17	12
Mg^{2+}	7	6	K	18	13
Ca^{2+}	32	26	Ca	13	9
Al	30.3	8.05	Ti	5	3
V	0.11	0.03	V	3	2
Cr	1.46	0.39	Cr	2	1
Mn	0.06	0.02	Mn	1	1
Fe	2.62	0.70	Fe	1	1
Ni	0.08	0.02	Ni	1	1
Cu	0.18	0.05	Cu	1	1
Zn	1.31	0.35	Zn	1	1
Cd	0.02	0.004	As	1	1
Sb	0.03	0.01	Se	1	1
Ba	0.10	0.03	Br	1	1
Pb	0.16	0.04	Rb	2	3
			Sr	2	3
			Pb	2	1

612

613

Table 2: Mean, standard deviation and percentage composition of water soluble ion and metal concentrations of Partisol daily data ($PM_{2.5}$ and $PM_{2.5-10}$) in Port Talbot.

Site	Fire Station (N=29)				Prince Street (N=12)				Dyffryn School (N=29)				Little Warren (N=29)			
	$PM_{2.5}$ ($\mu g/m^3$)		$PM_{2.5-10}$ ($\mu g/m^3$)		$PM_{2.5}$ ($\mu g/m^3$)		$PM_{2.5-10}$ ($\mu g/m^3$)		$PM_{2.5}$ ($\mu g/m^3$)		$PM_{2.5-10}$ ($\mu g/m^3$)		$PM_{2.5}$ ($\mu g/m^3$)		$PM_{2.5-10}$ ($\mu g/m^3$)	
Parameters	Mean ±SD	%	Mean ±SD	%	Mean ±SD	%	Mean ±SD	%	Mean ±SD	%	Mean ±SD	%	Mean ±SD	%	Mean ±SD	%
Mass	7.4[a] ±2.1	100	13.6[bc] ±11.7	100	9.2[b] ±1.7	100	16.7[c] ±10.5	100	7.3[a] ±3.0	100	8.3[a] ±4.9	100	6.5[a] ±2.5	10	9.3[ab] ±4.36	100
Cl^-	0.34[a] ±0.33	5	1.33[a] ±1.06	10	0.41[a] ±0.43	4	1.80[a] ±1.34	11	0.44[a] ±0.42	6	1.52[a] ±1.54	20	0.40[a] ±0.37	6	1.96[a] ±1.47	21
NO_3^-	0.62[a] ±0.49	8	0.45[a] ±0.27	3	0.52[a] ±0.41	6	0.47[a] ±0.35	3	0.95[a] ±0.81	13	1.03[b] ±1.58	15	0.95[a] ±0.74	15	0.81[ab] ±0.79	9
$nss\text{-}SO_4^{2-}$	1.91[ab] ±1.02	26	0.36[a] ±0.38	3	1.66[a] ±0.38	18	0.28[ab] ±0.26	2	2.29[ab]± 1.31	31	0.70[c] ±0.46	9	2.51[b] ± 1.23	39	0.57[bc] ±0.42	6
$ss\text{-}SO_4^{2-}$	0.09[a] ±0.05	1	0.21[a] ±0..13	2	0.08[a] ±0.05	1	0.27[ab] ±0.16	2	0.09[a] ±0.05	1	0.21[ab] ±0.15	3	0.12[b] ±0.05	2	0.31[b] ±0.19	3
Na^+	0.34[a] ±0.20	5	0.82[a] ±0.52	6	0.31[a] ±0.19	3	1.06[ab] ±0.62	6	0.34[a] ±0.21	5	0.87[ab] ±0.59	10	0.49[b] ±0.22	8	1.23[b] ±0.74	13
NH_4^+	0.68[a] ±0.53	9	0.07[a] ±0.06	<1	0.58[a] ±0.34	6	0.06[a] ±0.04	<1	0.75[a] ±0.65	10	0.07[a] ±0.09	2	0.82[a] ±0.65	13	0.14[b] ±0.11	2
K^+	0.11[a] ±0.01	2	0.08[a] ±0.07	1	0.14[a] ±0.09	2	0.09[a] ±0.08	1	0.10[a] ±0.07	1	0.08[a] ±0.06	1	0.15[a] ±0.10	2	0.12[a] ±0.07	1
Mg^{2+}	0.05[a] ±0.04	1	0.13[a] ±0.10	1	0.05[a] ±0.02	1	0.16[a] ±0.11	1	0.04[a] ±0.03	1	0.12[a] ±0.09	1	0.06[a] ±0.03	1	0.15[a] ±0.09	2
Ca^{2+}	0.15[a] ±0.13	2	0.80[b] ±0.77	6	0.11[a] ±0.07	1	0.91[b] ±0.77	5	0.10[a] ±0.15	1	0.41[a] ±0.45	5	0.15[a] ±0.17	2	0.45[a] ±0.37	5
Al*	128.9[b] ±34.3	2	142.6[b] ±58.5	1	109.6[a] ±7.9	1	140.8[ab] ±44.8	1	116.0[ab] ±16.1	2	110.6[a] ±34.1	1	117.9[ab] ±24.7	2	123.6[ab] ±48.3	1
V*	0.52[a] ±0.23	<1	0.53[bc] ±0.42	<1	0.50[a] ±0.23	<1	0.64[c] ±0.34	<1	0.49[a] ±0.21	<1	0.41[a] ±0.32	<1	0.59[a] ±0.28	<1	0.31[ab] ±0.18	<1
Cr*	3.48[a] ±1.52	<1	2.89[a] ±1.52	<1	4.76[a] ±2.04	<1	3.67[a] ±1.16	<1	2.78[a] ±1.55	<1	3.14[a] ±1.49	<1	4.52[a] ±3.19	<1	2.97[a] ±1.49	<1
Mn*	5.72[a] ±7.6	<1	26.47[bc] ±35.1	<1	12.76[b] ±11.8	<1	29.52[c] ±27.0	<1	7.03[a] ±10.7	<1	12.65[ab] ±13.8	<1	3.84[a] ±4.8	<1	10.0[a] ±12.5	<1
Fe*	173[a] ±237	2	1196[b] ±1642	9	290[b] ±229	3	1439[b] ±1485	9	142[a] ± 147	2	421[a] ±433	5	104[a] ± 108	2	520[a] ±669	6
Ni*	0.20[a] ±0.33	<1	0.19[ab] ±0.22	<1	0.16[a] ±0.27	<1	0.24[b] ±0.22	<1	0.12[a] ±0.17	<1	0.11[a] ±0.15	<1	0.12[a] ±0.20	<1	0.14[ab] ±0.22	<1
Cu*	1.89[a] ±1.21	<1	2.05[b] ±0.87	<1	2.90[b] ±1.51	<1	3.20[c] ±1.69	<1	1.42[a] ±0.90	<1	1.45[ab] ±1.0	<1	1.38[a] ±1.26	<1	1.12[a] ±0.70	<1
Zn*	43.0[a] ±85.55	1	7.30[a] ±8.03	<1	67.97[a] ±165.8	1	16.26[a] ±30.87	<1	71.51[a] ±117.2	1	20.31[a] ±26.48	<1	33.98[a] ±86.7	1	8.30[a] ±17.71	<1
Cd*	0.26[a] ±0.55	<1	0.02[a] ±0.06	<1	0.88[a] ±2.11	<1	0.06[a] ±0.12	<1	0.69[a] ±1.34	<1	0.08[a] ±0.15	<1	0.31[a] ±0.52	<1	0.03[a] ±0.09	<1
Sb*	0.57[a] ±0.52	<1	0.36[b] ±0.21	<1	0.99[b] ±1.14	<1	0.66[c] ±0.34	<1	0.38[a] ±0.32	<1	0.13[a] ±0.14	<1	0.53[a] ±0.71	<1	0.11[a] ±0.22	<1
Ba*	1.04[b] ±0.5	<1	3.03[b] ±2.06	<1	1.69[c] ±0.75	<1	4.04[c] ±2.32	<1	0.49[a] ±0.25	<1	1.41[a] ±0.81	<1	0.34[a] ±0.26	<1	1.15[a] ±0.70	<1
Pb*	4.42[a] ±3.88	<1	2.04[ab] ±2.40	<1	7.65[a] ±7.98	<1	2.95[b] ±4.20	<1	8.12[a] ±9.27	<1	1.44[a] ±1.51	<1	7.02[a] ±6.86	<1	1.32[a] ±1.43	<1

Superscripts of the same letter on the rows are not significantly different at $p<0.05$, * units in ng/m^3

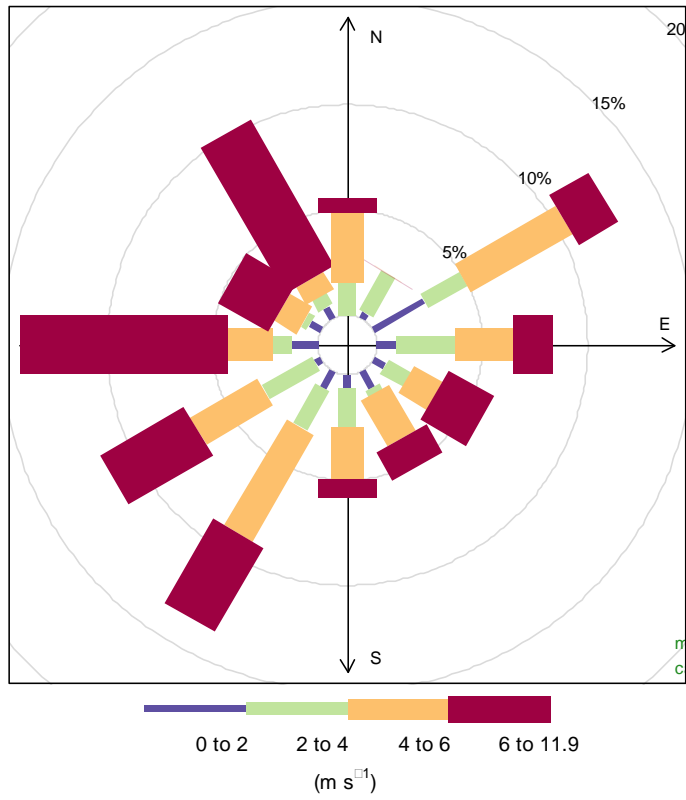$nss\text{-}SO_4^{2-}$ calculated following Sciare et al. (2003)

621

622
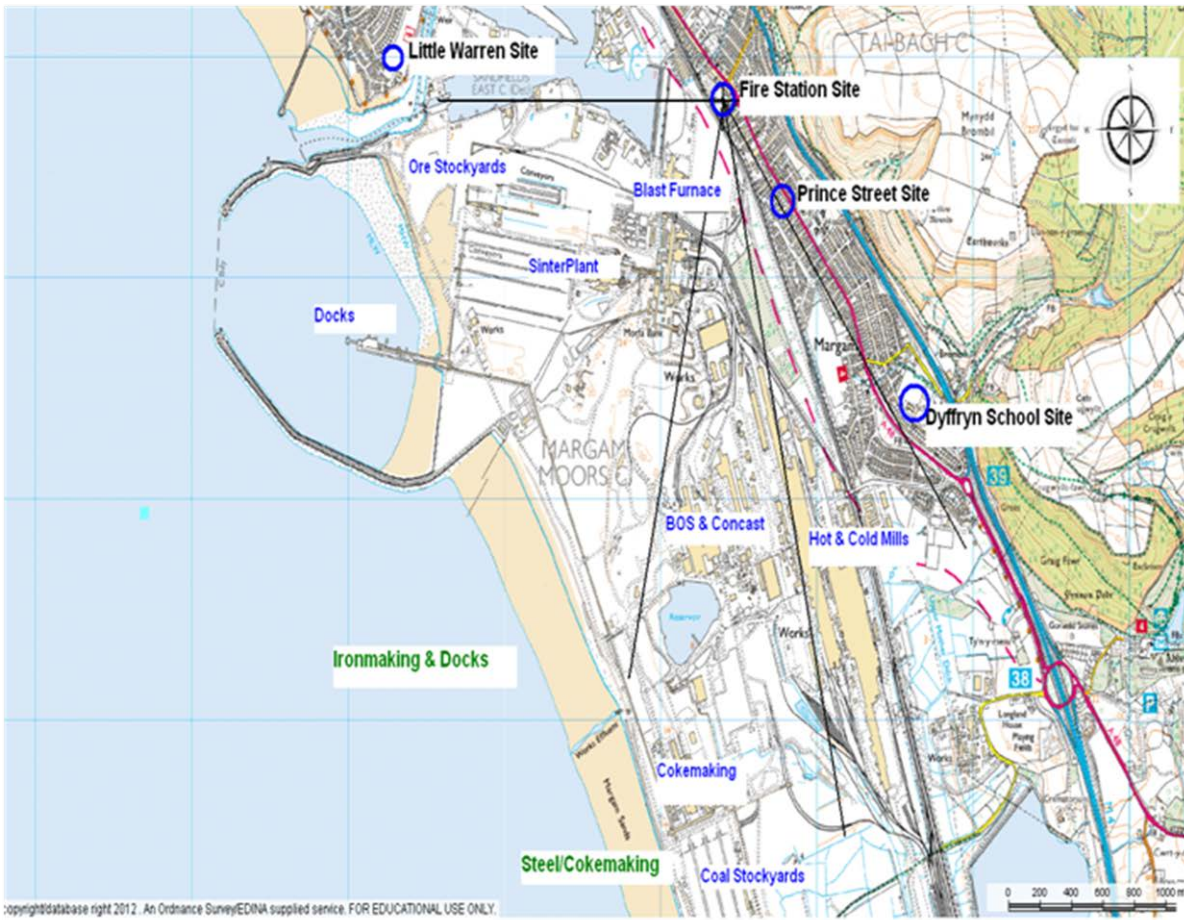
Figure 1: Map of study area.

624

625

Figure 2: Average wind rose for Margam station (Fire Station site) in Port Talbot during the campaign period.
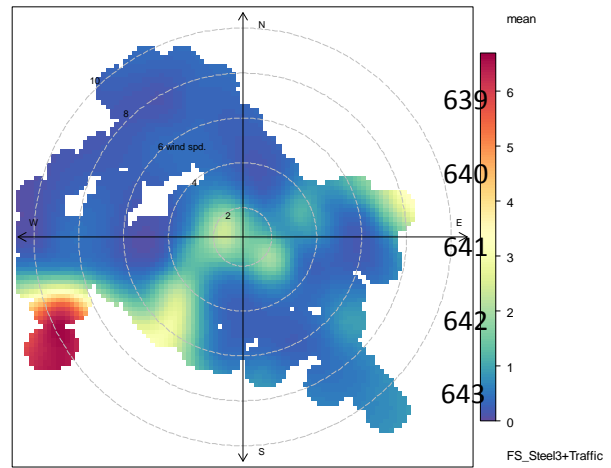
Figure 3: 6-Factor solution resolved by ME-2 for hourly PM10 (i.e. fine + coarse PM fraction) collected at Little Warren (on the left) and Fire Station (on the right). Chemical profiles are represented as bars (in arbitrary units) and the explained variation values (EVF) as dots.
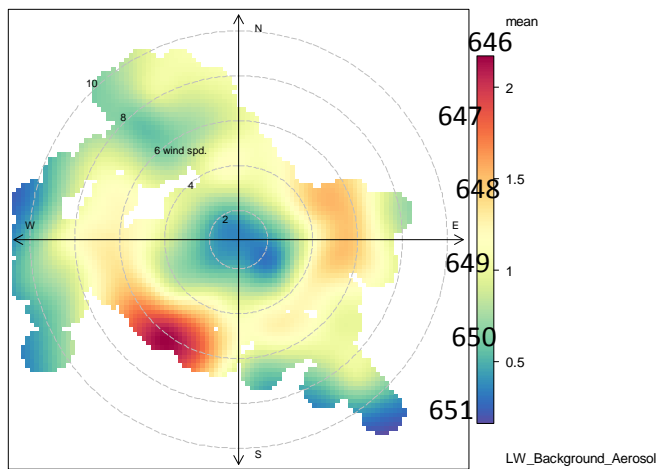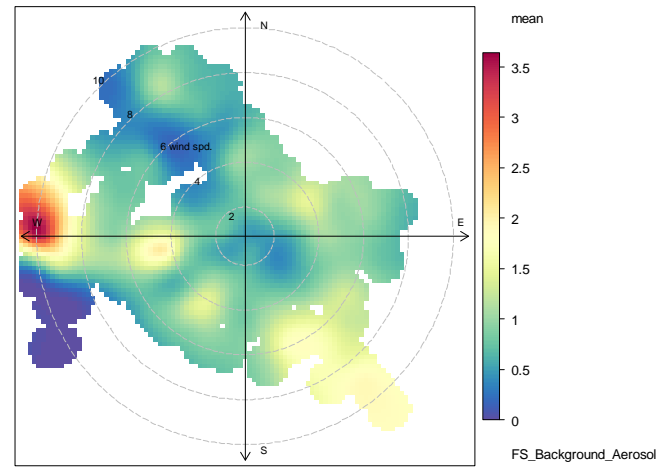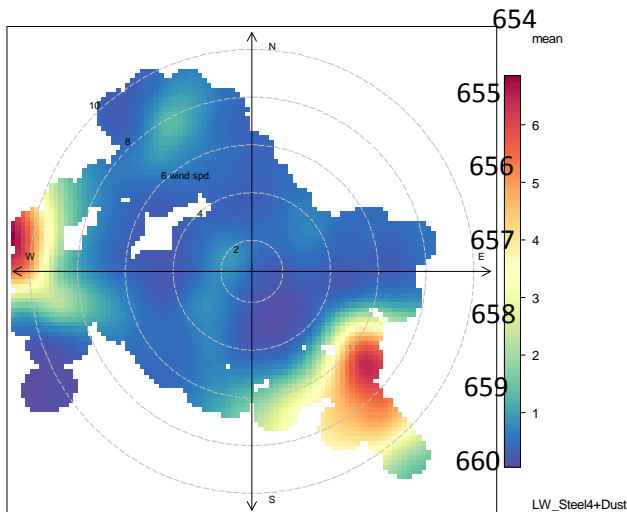
27

636 (4a)

637 (4b)

638 (4c)
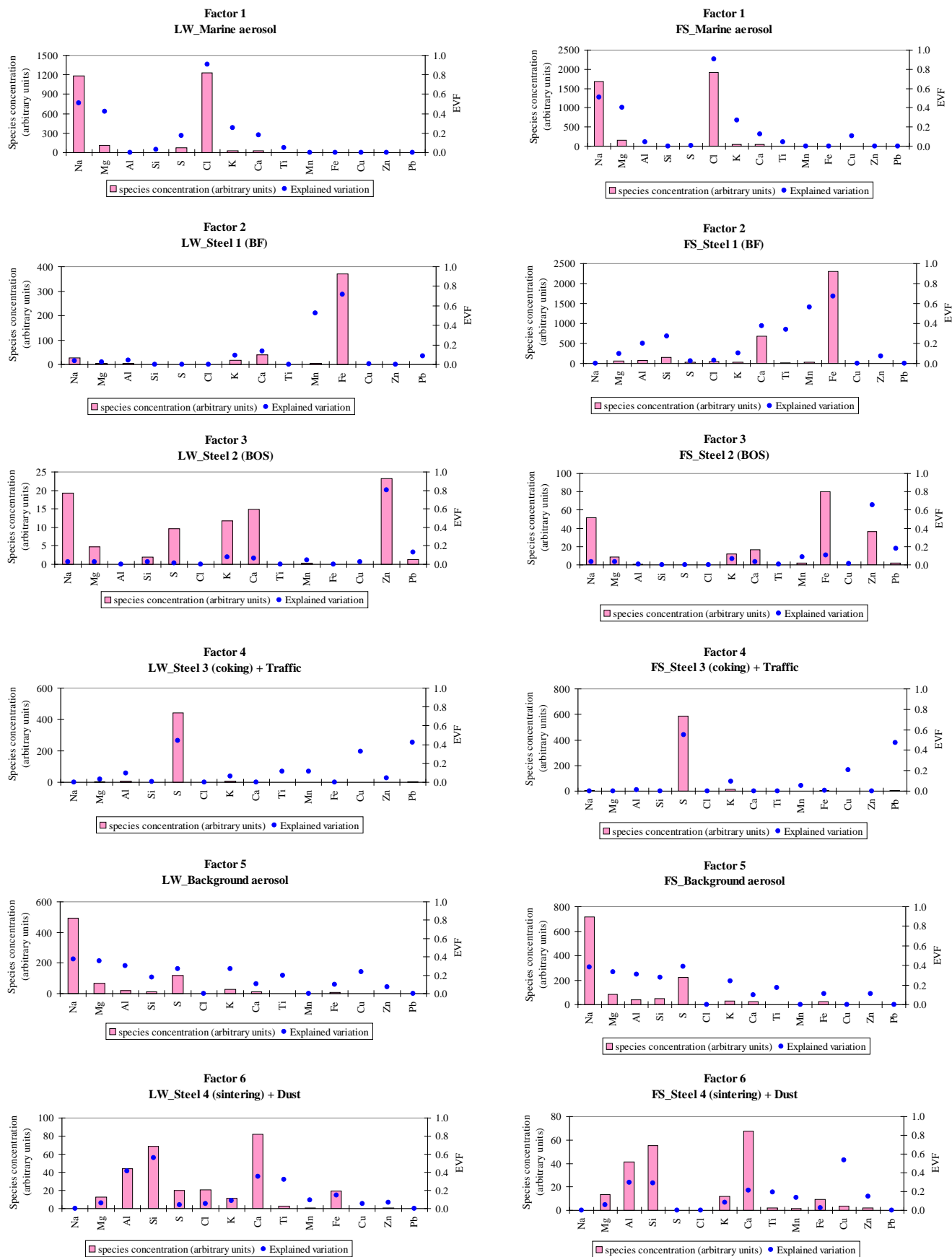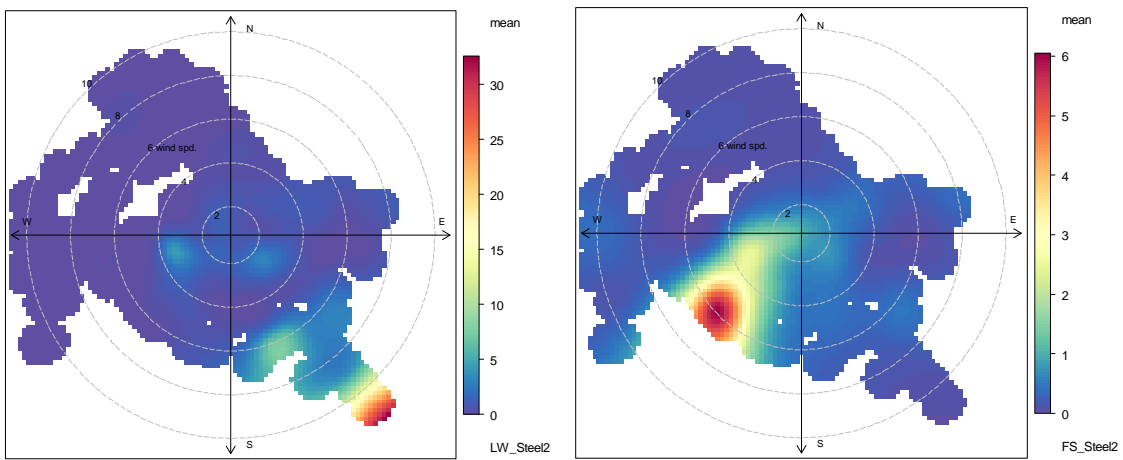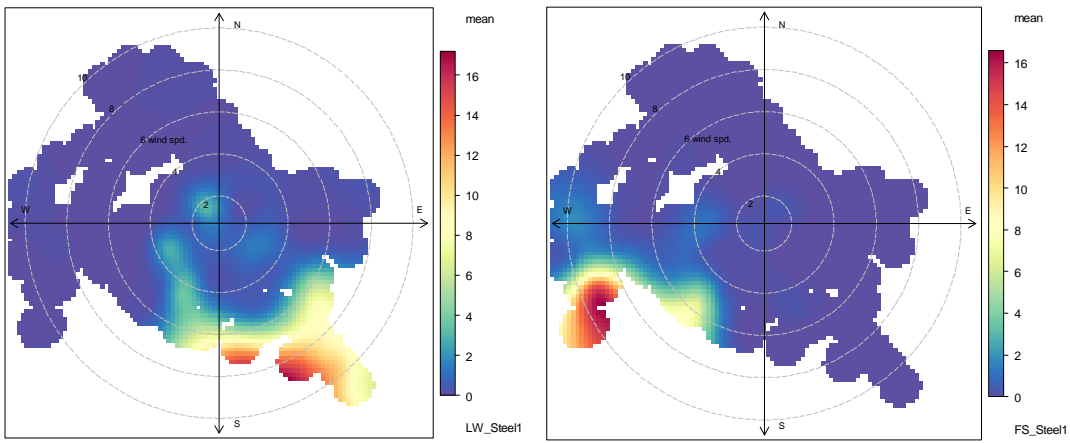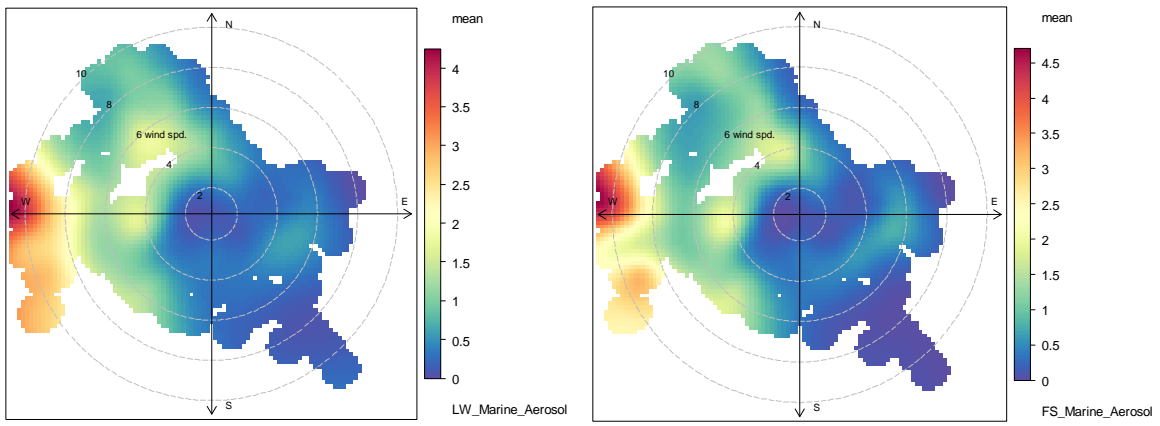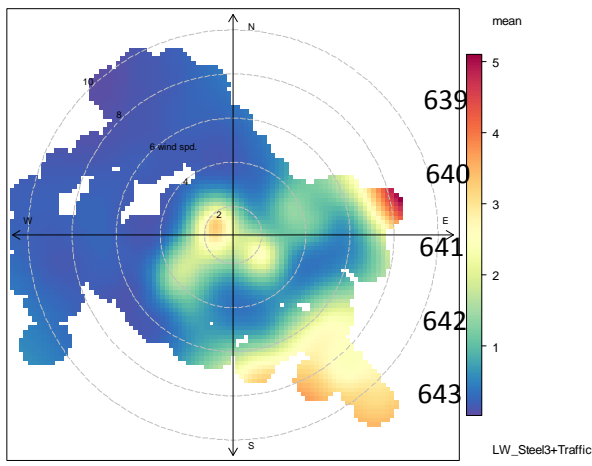
644

(4d)

645

652

653

(4e)

661
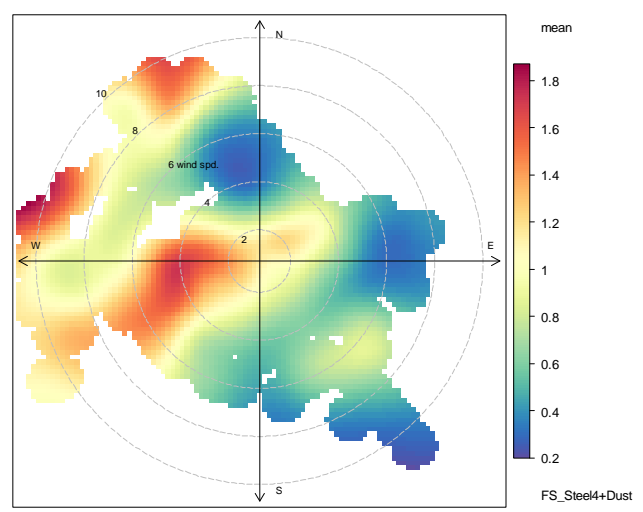
662

(4f)

Figure 4 : Bi-variate polar plots of hourly data in ME-2 factor contributions. (a) Marine aerosol; (b) Steel 1; (c) Steel 2; (d) Secondary + Traffic; (e) Background aerosol; (f) Steel 4 + Dust. LW site on the left; FS on the right.
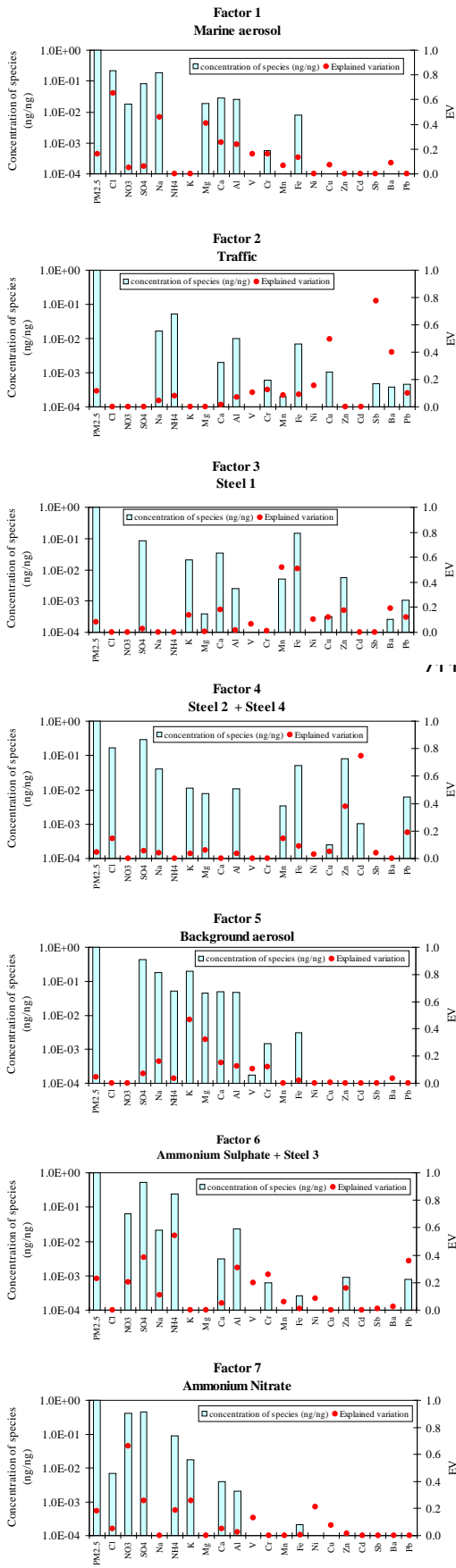
666

667

668
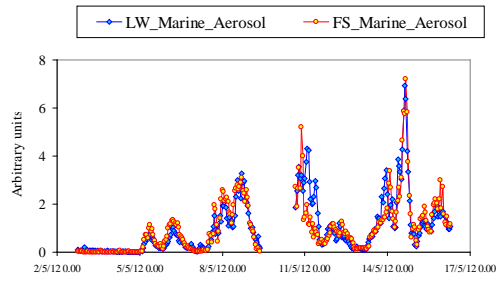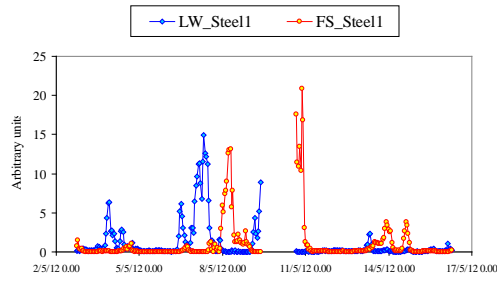
669

670

671
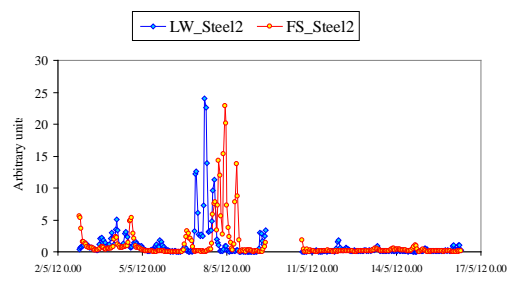
672

673

674
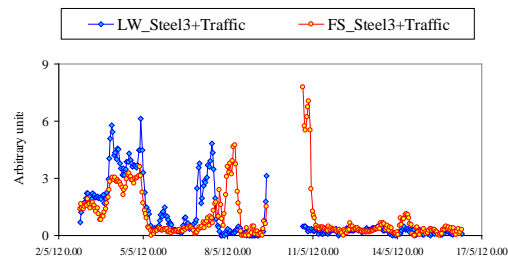
675

676

677

678

679

680

681

682

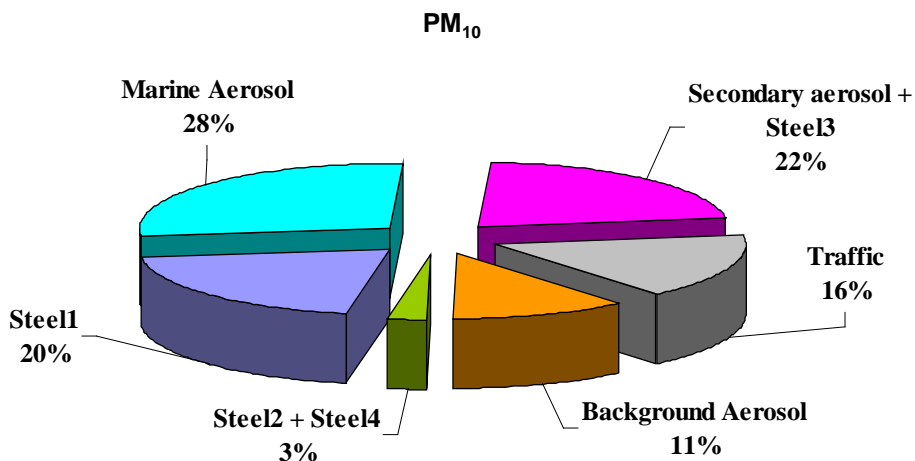**Figure 5:** Hourly temporal patterns of factor contributions obtained in the ME-2 6-factor solution.

684
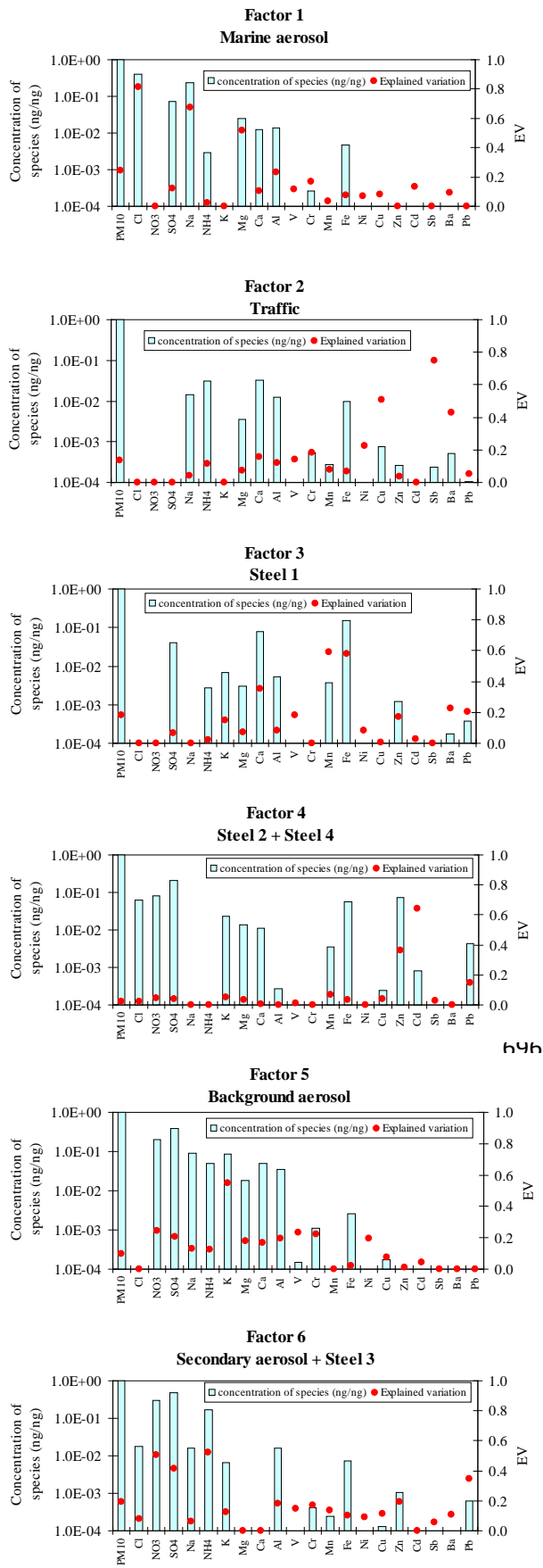
Figure 6a: 6-Factor solution resolved by ME-2 for PM$_{10}$ (daily data) in the steelworks area. Chemical profiles are represented as bars (in ng/ng) and the explained variation as dots.

Figure 6b: 7-Factor solution resolved by ME-2 for PM$_{2.5}$ (daily data) in the steelworks area. Chemical profiles are represented as bars (in ng/ng) and the explained variation as dots.
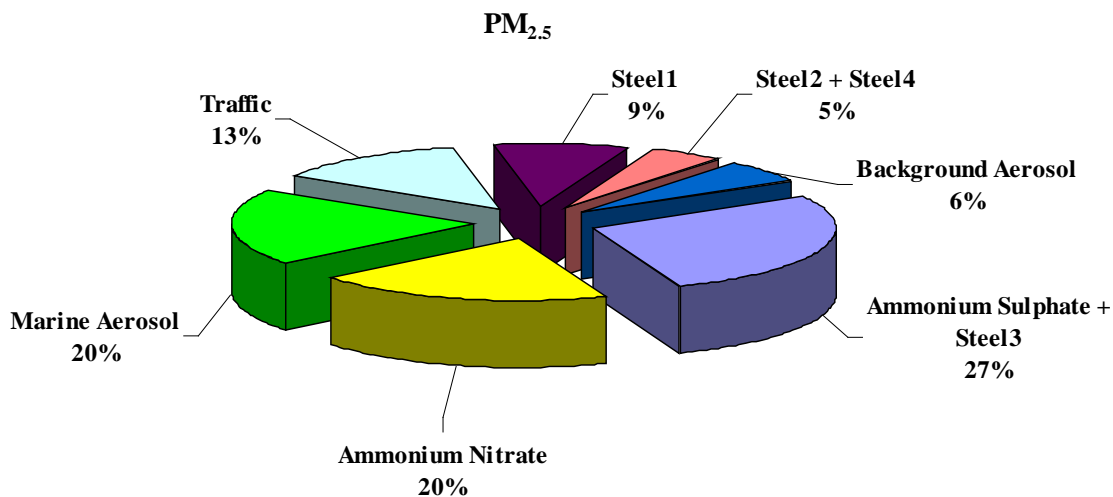
32

Figure 6c: 6-Factor solution resolved by ME-2 for PM$_{2.5-10}$ (daily data) in the steelworks area. Chemical profiles are represented as bars (in ng/ng) and the explained variation as dots.

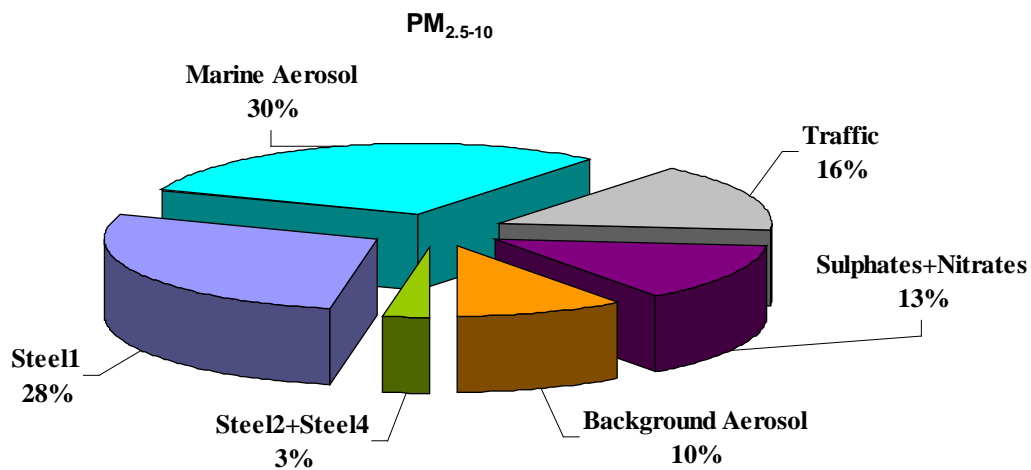**PM$_{10}$**

742

743 **Figure 7a:** Source apportionment for PM$_{10}$ (daily data) in the steelworks area.

744

PM$_{2.5}$

745

746 **Figure 7b:** Source apportionment for PM$_{2.5}$ (daily data) in the steelworks area.

PM$_{2.5-10}$

747

748 **Figure 7c:** Source apportionment for PM$_{2.5-10}$ (daily data) in the steelworks area.